On the Phase Transition of Bis(pyridinium)hexachlorometallates, $(C_5H_5NH)_2[MCl_6]$, M = Sn, Te, Pb, Pt. An X-Ray and ^{35}Cl NQR Study

Dirk Borchers* and Alarich Weiss

Institut für Physikalische Chemie III, Technische Hochschule Darmstadt, West Germany

Z. Naturforsch. **42 a**, 739–748 (1987); received April 1, 1987

A phase transition has been observed in bis(pyridinium)hexachlorometallates $(C_5H_5NH)_2[M^{IV}Cl_6]$, M = Sn, Te, Pb, Pt. The crystal structure of the low temperature phase II of the salt with M = Sn was determined, space group C_i^1-$P\bar{1}$, $Z = 1$ ($a = 734.1$ pm, $b = 799.0$ pm, $c = 799.7$ pm, $\alpha = 83.229°$, $\beta = 65.377°$, $\gamma = 84.387°$, $T = 297$ K). The four compounds are isotypic in phase II as well as in the high temperature phase I (C_{2h}^2-B2/m, $Z = 2$) for which the crystal structure is known for M = Te. The lattice constants of all compounds (both phases) are given. The temperature dependence of the ^{35}Cl NQR spectrum was investigated. The three line ^{35}Cl NQR spectrum is in agreement with the crystal structure. The dynamics of the pyridinium ring shows up in a fade out of part of the ^{35}Cl NQR spectrum. The influence of H ↔ D exchange on ^{35}Cl NQR is studied and an assignment of $\nu(^{35}Cl) \leftrightarrow Cl^{(1)}$ is proposed. The nature of the phase transition $P\bar{1}$ ($Z = 1$) ↔ B2/m ($Z = 2$) is discussed.

Introduction

Many hexachlorometallates with the composition $(A^I)_2MCl_6$ and $A^{II}MCl_6 \cdot 6\,H_2O$ have been studied by $^{35,37}Cl$ NQR spectroscopy during the last twenty years; for a review see [1, 2]. Preferentially the elements M = Sn, Pb, Se, Te as the central atom of the complex ion $[MCl_6]^{2-}$ were of interest, as were the transition elements M = Pt, Pd. The alkali metal ions $A^I = K^+$, Rb^+, Cs^+ and the ammonium ions $A^I = NH_4^+$, $CH_3NH_3^+$, ..., $N(CH_3)_4^+$ found particular attention. Due to the sphericity of the alkali metal ions highly symmetric crystal structures are expected for $(A^I)_2MCl_6$, and the literature confirms this expectation: The K_2PtCl_6-type structure, O_h^5-Fm 3 m ($Z = 4$), is often observed.

With partially substituted ammonium ions, such as CH_3NH_3, ..., hydrogen bonds $-N-H \ldots Cl-M$ have to be considered. Indeed, a lowering of the solid state symmetry of the complex ion $[MCl_6]^{2-}$ from the regular octahedron is common with simple ammonium salts A_2MCl_6, A being $CH_3NH_3^+$, $(CH_3)_2NH_2^+$ and $(CH_3)_3NH^+$. Additionally, the non-sphericity of the substituted ammonium ions leads to consequences for the octahedral symmetry of $[MCl_6]^{2-}$. Both, the overall dynamics of the substituted ammonium ions in the lattice and the substitutional group dynamics, e.g. of the CH_3-group, may counteract the decrease in symmetry initiated by the hydrogen bond.

"Large" cations A^+ or A^{2+}, having low symmetry by nature and, additionally, the power of forming hydrogen bonds to the Cl-atoms in $[MCl_6]^{2-}$ found our interest recently. We have reported ^{35}Cl NQR work and crystal structure studies on a group of salts $(H_3N(CH_2)_2NH_3)^{2+}[MCl_6]^{2-}$, M = Sn, Te, Pb, Pt [3] and Brill and Welsh [4] have reported some ^{35}Cl NQR frequencies at room temperature for $(C_5H_5NH)_2[MCl_6]$, $M = Sn^{IV}$, Te^{IV}, Pb^{IV}. As much as the crystal structures of bis(pyridinium)hexachlorometallates(IV) is concerned, Aynsley and Hazell [5] performed single crystal X-ray work on $(C_5H_5NH)_2[TeCl_6]$, including a determination of the unit cell dimensions and the space group; Khodadad et al. determined the room temperature crystal structure of this compound [6]. Values of $d(hkl)$ for bis(pyridinium)hexachloroplatinate can be found in [7].

The pyridinium ion $[C_5H_5NH]^+$ is an interesting cation with respect to its behaviour in the lattice and the hydrogen bond interactions with the anions of the salt. One may expect strong librational

* Part of Dr.-Ing. thesis of Dirk Borchers, D 17, Technische Hochschule Darmstadt.

Reprint requests to Prof. Dr. Al. Weiss, Institut für Physikalische Chemie III, Technische Hochschule Darmstadt, Petersenstraße 20, D-6100 Darmstadt.

0932-0784 / 87 / 0700-0739 $ 01.30/0. – Please order a reprint rather than making your own copy.

Dieses Werk wurde im Jahr 2013 vom Verlag Zeitschrift für Naturforschung in Zusammenarbeit mit der Max-Planck-Gesellschaft zur Förderung der Wissenschaften e.V. digitalisiert und unter folgender Lizenz veröffentlicht: Creative Commons Namensnennung-Keine Bearbeitung 3.0 Deutschland Lizenz.

This work has been digitalized and published in 2013 by Verlag Zeitschrift für Naturforschung in cooperation with the Max Planck Society for the Advancement of Science under a Creative Commons Attribution-NoDerivs 3.0 Germany License.

Zum 01.01.2015 ist eine Anpassung der Lizenzbedingungen (Entfall der Creative Commons Lizenzbedingung „Keine Bearbeitung") beabsichtigt, um eine Nachnutzung auch im Rahmen zukünftiger wissenschaftlicher Nutzungsformen zu ermöglichen.

On 01.01.2015 it is planned to change the License Conditions (the removal of the Creative Commons License condition "no derivative works"). This is to allow reuse in the area of future scientific usage.

Table 1. Habitus, colour, decomposition temperature T_d, and chemical analysis (C, H, N) of bis(pyridinium)hexachlorometallates $(C_5H_5NH)_2[MCl_6]$, M = Sn, Te, Pb, Pt.

M	Colour	Habitus	Lit.	T_d/K	Chemical analysis (% weight)					
					C_{calc}	(C_{found})	N_{calc}	(N_{found})	H_{calc}	(H_{found})
Sn	white	plates	[12]	571	24.42	(24.36)	5.70	(5.68)	2.44	(2.34)
Te	yellow	plates	[13]	530	23.99	(23.86)	5.60	(5.54)	2.40	(2.29)
Pb	yellow	plates	[14]	515	20.69	(20.63)	4.83	(4.80)	2.07	(1.92)
Pt	orange	plates	[15]	501	21.13	(19.28)	4.93	(4.46)	2.11	(2.03)

motions of the ion around its pseudo sixfold axis. On the other hand, the hydrogen bond N–H ... X should be rather strong due to the rather strong base character of pyridine. A number of crystal structure investigations shows the pyridinium ion as an almost regular hexagon; sometimes the nitrogen atom can not be fixed to a certain position in the ring $[C_5H_5NH]^+$, for example in pyridinium iodide [8] and pyridinium salts with hexafluoro group-V-anions [9]. Distinct nitrogen positions have been found, however, in the ordered crystal structures of pyridinium nitrate [10] and pyridinium chloride [11]. In these solids the shortest distances ring atom-X have been interpreted as the hydrogen bonds N–H ... Cl.

In the present investigation ^{35}Cl NQR studies on the bis(pyridinium)hexachlorometallates $(C_5H_5NH)_2[MCl_6]$, M = Sn, Te, Pb, Pt are reported together with crystal structure data.

Experimental

Preparation of the Compounds

Bis(pyridinium)hexachlorostannate, $(C_5H_5NH)_2[SnCl_6]$, was prepared by mixing the aqueous solution of pyridinium hydrochloride with stoichiometric amounts of a solution of $SnCl_4$ in 2*n*-HCl. The white crystalline product formed was recrystallized from dilute hydrochloric acid. The N-deuterated compound $(C_5H_5ND)_2[SnCl_6]$ was prepared by dissolving the protonated species in D_2O, evaporating the D_2O, and repeating this procedure several times. The ring deuterated bis(pyridinium)-hexachlorostannate $(C_5D_5NH)_2[SnCl_6]$ was obtained in the same way as the protonated compound using C_5D_5N, respectively.

The bis(pyridinium)hexachlorotellurate was synthesized by mixing an aqueous solution of pyridinium hydrochloride with a solution of H_2TeCl_6 in concentrated HCl, prepared by dissolving TeO_2 in concentrated HCl. The platinum compound was obtained similarly by using $H_2PtCl_6 \cdot 4.5\,H_2O$. Finally for the preparation of $(C_5H_5NH)_2[PbCl_6]$, lead tetraacetate $[Pb(OOCCH_3)_4]$, was dissolved in concentrated hydrochloric acid. A stoichiometric amount of pyridinium hydrochloride in conc. HCl was added. The yellow precipitate was filtered off and redissolved in concentrated hydrochloric acid while chlorine gas was passed through the solution. Chlorine gas was also passed through the solution during cooling whereby the compound precipitated. The crystalline solid was filtered off immediately thereafter and dried over $CaCl_2$ in a dessicator. The yields for all preparations described above were nearly quantitative. All chemicals used for the preparative work were form commercial source and of laboratory grade. In Table 1 the chemical analysis, habitus of the crystalline compounds, colour, and melting points are listed.

Crystal Structure Analysis

The crystal structure of bis(pyridinium)hexachlorostannate was studied in detail at room temperature by single crystal technique. In Table 2 the experimental conditions and parameters are listed together with crystallographic data (lattice constants, space group etc.). According to the transition points of the bis(pyridinium)hexachlorometallates, which have been found from ^{35}Cl NQR spectroscopy (see Table 8), we determined the structure of the low temperature phase of $(C_5H_5NH)_2[SnCl_6]$, Phase II, while Khodadad et al. [6] investigated the high temperature phase of $(C_5H_5NH)_2[TeCl_6]$. By Debye-Scherrer technique X-ray powder diffraction diagrams were taken for all compounds in question using a position sensitive detector and CoKα-

Table 2. Experimental conditions for the structure determination and crystal structure data of bis(pyridinium)-hexachlorostannate, $(C_5H_5NH)_2[SnCl_6]$, phase II. In this table, as in the following ones, the error is given in parentheses.

Crystal habitus, size	prism (0.15 × 0.25 × 0.6) mm³
Diffractometer	Stoe-Siemens AED-2
Wavelength pm (MoKα)	71.073
Monochromator	Graphit (002)
T/K	297
Absorption coefficient μ/m^{-1}	2272
Scan	$2\vartheta/\omega$
$(\sin\vartheta/\lambda)_{max}$/pm	0.007035
Number of reflexions measured	2463
Symmetry independent reflexions	2451
Reflexions considered	2436
Number of free parameters	107
F(000)	238
R(F)	0.020
Rw(F)	0.021
Point positions	all atoms in 2 i $x, y, z; \bar{x}, \bar{y}, \bar{z}$
Lattice constants a/pm	734.1(2)
b/pm	799.0(2)
c/pm	799.7(2)
α/°	83.299(5)
β/°	65.377(5)
γ/°	84.387(5)
Volume of the unit cell $V \cdot 10^{-6}$/(pm)³	422.8
Space group	$C_i^1-P\bar{1}$
Formula units per unit cell Z	1
φ_{calc}/(Mg m^{-3})	1.930 (T = 297 K)
φ_{exp}/(Mg m^{-3})	1.92 (T = 293 K)

radiation (λ = 178.81 pm). From the results of the crystal structure determination of bis(pyridinium)-hexachlorostannate (low temperature phase II) and the bis(pyridinium)hexachlorotellurate [6] (high temperature phase I) theoretical patterns were calculated and have been used for the calibration of the position sensitive detector. To generate the different temperatures, the sample was placed in a gas stream. The temperature accuracy is ± 2 K. We could not determine the crystal parameters of the low temperature phase II of $(C_5H_5NH)_2[TeCl_6]$, because of low transition temperature T_c, which is outside of the range of the powder diffractometer available to us.

^{35}Cl NQR

^{35}Cl NQR of the bis(pyridinium)hexachloro-metallates was studied as a function of temperature in the range 77 ≦ T/K ≦ temperature at which the lines fade out. A superregenerative NQR spectrometer was used. To get the wanted temperatures at the sample site different methods were employed:

Temperature range	Method	Estimated error in T
77 K	liquid nitrogen bath	± 0.5 K
100 ≦ T/K ≦ 200	nitrogen gas stream	± 0.8 K
200 ≦ T/K ≦ 300	methanol bath	± 0.1 K
300 ≦ T/K ≦ 350	oil bath	± 0.5 K

All temperatures were measured with copper-constantan thermocouples. The accuracy in determining the ^{35}Cl NQR frequency is ± 5 kHz and the limitation is due to the line widths.

Results

X-Ray Diffraction

The X-ray structure analysis of bis(pyridinium)-hexachlorostannate (low temperature phase II) started with a Fourier syntheses with Sn at 0, 0, 0, from which the positions of the other atoms followed. After refinement by least squares cycles a difference Fourier map was calculated. The positions of the hydrogens were taken therefrom. Isotropic temperature factors were refined for the hydrogens, anisotropic ones for the other atoms. The resulting reliability factors and conditions for the single crystal structure determination of bis-(pyridinium)hexachlorostannate and the results are listed in Table 2. In Table 3 the positional and thermal parameters of the crystal structure are given. In Table 4 the bond distances and bond angles are listed for this compound. From powder diffraction diagrams the unit cell dimensions of the corresponding bis(pyridinium)hexachlorometallates were determined. The cell constants of all compounds in the high (I) and low (II) temperature phase are given in Table 5.

^{35}Cl NQR

In Fig. 1 the ^{35}Cl NQR frequencies of bis-(pyridinium)hexachlorostannate are shown as a

Table 3. Positional and thermal parameters of bis(pyridinium)hexachlorostannate, $(C_5H_5NH)_2[SnCl_6]$, low temperature phase II. The temperature factor is of the form

$$T = \exp\{-2\pi^2(U_{11}\,h^2\,a^{*2} + U_{22}\,k^2\,b^{*2} + U_{33}\,l^2\,c^{*2} + 2\,U_{12}\,h\,k\,a^*\,b^* + 2\,U_{13}\,h\,l\,a^*\,c^* + 2\,U_{23}\,k\,l\,b^*\,c^*)\}\,.$$

The U_{ij} are given in $(pm)^2$. U is the isotropic mean for the hydrogen atoms.

Atom	x/a	y/b	z/c	U_{11}, U	U_{22}	U_{33}	U_{12}	U_{13}	U_{23}
Sn	0	0	0	311(1)	265(1)	321(1)	−32(1)	−78(1)	1(1)
$Cl^{(1)}$	−0.0748(1)	0.2936(1)	−0.0755(1)	529(3)	303(2)	543(3)	8(2)	−166(2)	36(2)
$Cl^{(2)}$	0.2922(1)	−0.0018(1)	−0.2892(1)	447(2)	440(3)	402(2)	−83(2)	11(2)	−56(2)
$Cl^{(3)}$	0.2050(1)	0.0922(1)	0.1457(1)	565(3)	455(3)	558(3)	−108(2)	−305(3)	11(2)
N	0.4323(4)	0.7185(3)	0.2552(3)	764(14)	434(10)	642(13)	−203(10)	−374(12)	118(9)
$C^{(1)}$	0.2737(4)	0.7294(3)	0.4142(4)	788(17)	457(12)	668(16)	80(12)	−419(14)	−136(11)
$C^{(2)}$	0.1986(4)	0.5878(4)	0.5200(4)	501(13)	810(18)	482(13)	−11(12)	−182(10)	−33(12)
$C^{(3)}$	0.2847(4)	0.4349(3)	0.4580(4)	637(14)	462(13)	730(17)	−173(11)	−353(13)	192(11)
$C^{(4)}$	0.4472(4)	0.4287(3)	0.2932(4)	616(14)	443(12)	730(16)	67(10)	−335(13)	−77(11)
$C^{(5)}$	0.5221(4)	0.5736(4)	0.1921(4)	492(12)	656(15)	515(13)	−81(10)	−187(10)	3(11)
$H^{(N)}$	0.4659(41)	0.8212(36)	0.2019(39)	600					
$H^{(C,1)}$	0.2260(40)	0.8328(35)	0.4427(37)	600					
$H^{(C,2)}$	0.1003(40)	0.5967(35)	0.6161(39)	600					
$H^{(C,3)}$	0.2423(40)	0.3449(37)	0.5125(40)	600					
$H^{(C,4)}$	0.5099(41)	0.3292(35)	0.2556(37)	600					
$H^{(C,5)}$	0.6356(39)	0.5724(31)	0.0688(31)	600					

Table 4. Intra- and interionic bond distances and bond angles of $(C_5H_5NH)_2[SnCl_6]$, phase II.

Intraionic	d/pm	Intraionic	Angle/degree
$Sn-Cl^{(1)}$	242.0(1)	$Cl^{(1)}-Sn-Cl^{(2)}$	89.7(1)
$Sn-Cl^{(2)}$	241.5(1)	$Cl^{(1)}-Sn-Cl^{(3)}$	91.2(1)
$Sn-Cl^{(3)}$	245.9(1)	$Cl^{(2)}-Sn-Cl^{(3)}$	90.5(1)
$C^{(1)}-C^{(2)}$	134.5(4)	$C^{(1)}-C^{(2)}-C^{(3)}$	119.0(2)
$C^{(2)}-C^{(3)}$	136.7(4)	$C^{(2)}-C^{(3)}-C^{(4)}$	119.7(2)
$C^{(3)}-C^{(4)}$	136.2(4)	$C^{(3)}-C^{(4)}-C^{(5)}$	119.9(2)
$C^{(4)}-C^{(5)}$	135.3(4)	$C^{(4)}-C^{(5)}-N$	118.6(2)
$C^{(5)}-N$	132.0(4)	$C^{(5)}-N-C^{(1)}$	123.2(2)
$C^{(1)}-N$	132.4(4)	$N-C^{(1)}-C^{(2)}$	119.6(2)
N−H	88(3)		
$C^{(1)}-H$	88(3)		
$C^{(2)}-H$	81(3)		
$C^{(3)}-H$	81(3)		
$C^{(4)}-H$	90(3)		
$C^{(5)}-H$	99(3)		
$Cl^{(1)}\ldots Cl^{(2)}$	341.0(2), shortest		
$Cl^{(1)}\ldots Cl^{(3)}$	348.8(2), longest		
Interionic	d/pm		
$N\ldots Cl^{(1)}$	349.1(3)		
$N\ldots Cl^{(2)}$	328.6(3)		
$N\ldots Cl^{(3)}$	347.7(3)		
$Cl^{(1)}\ldots Cl^{(1)}$	403.7(2), shortest		

function of temperature. In Figs. 2–4 $\nu(^{35}Cl)$ is plotted for the corresponding hexachlorotellurate, hexachloroplumbate and hexachloroplatinate. N-deuteration $(C_5H_5ND)^+$ or ring-deuteration $(C_5D_5NH)^+$ of the cation shift the ^{35}Cl resonance frequencies and the transition temperatures slightly.

To rationalize the NQR spectra the experimental data was approximated by a power series

$$\nu(T) = \sum a_i\,T^i.$$

The coefficients of this power series are listed in Table 6 and in Table 7 resonance frequencies are given at selected temperatures. From the curves $\nu(^{35}Cl) = f(T)$, see Figs. 1–4, the phase transition temperatures T_c were extracted. They are listed in Table 8.

Discussion

Crystal Structure

The crystal structure of bis(pyridinium)hexachlorostannate, phase II, shows $[SnCl_6]^{2-}$ octahedra centered with the Sn-atom at the corners of the unit cell in 0, 0, 0. The distortion of the octahedra is only slight, $\langle d(Sn-Cl)\rangle = 243 \pm 3$ pm, $\langle \sphericalangle(Cl-Sn-Cl)\rangle = 90.0° \pm 1.2°$, see Table 4. The two cations $(C_5H_5NH)^+$ fill the free space in the interior of the cell and they are connected by the center of symmetry at $\frac{1}{2}, \frac{1}{2}, \frac{1}{2}$. In Fig. 5 the crystal structure of $(C_5H_5NH)_2[SnCl_6]$, phase II, is shown in projection along ***b***. It is seen that each pyridinium cation is connected by a trifurcated hydrogen bond to two neighbouring $[SnCl_6]$ octahedra. The hydrogen bond distances and angles are listed in Table 9. One of these hydrogen bond directions points to an atom

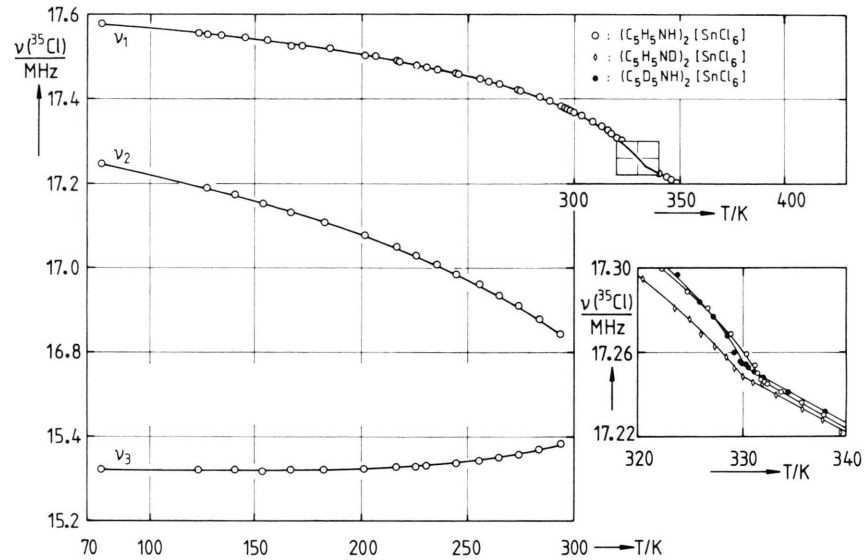

Fig. 1. ^{35}Cl NQR frequencies of bis(pyridinium)hexachlorostannate, $(C_5H_5NH)_2[SnCl_6]$, $(C_5H_5ND)_2[SnCl_6]$, and $(C_5D_5NH)_2[SnCl_6]$ as functions of temperature. The region near T_c is shown in the inset.

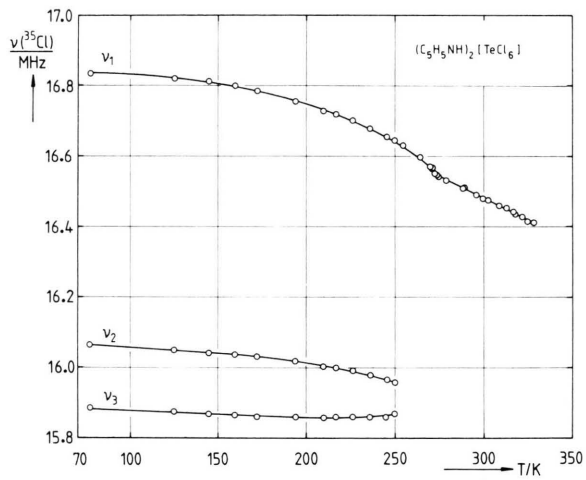

Fig. 2. ^{35}Cl NQR frequencies of bis(pyridinium)hexachlorotellurate, $(C_5H_5NH)_2[TeCl_6]$, vs. temperature.

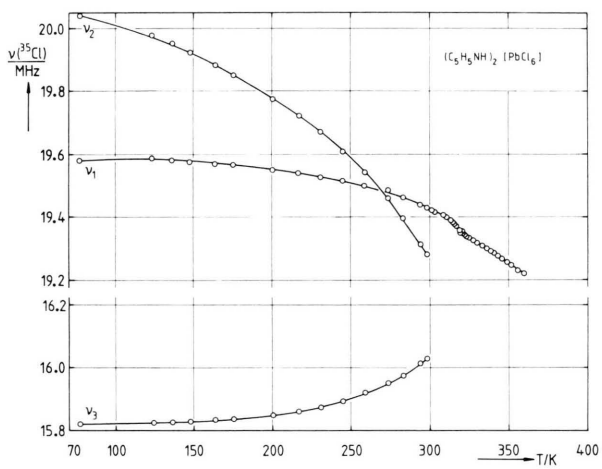

Fig. 3. ^{35}Cl NQR frequencies of bis(pyridinium)hexachloroplumbate, $(C_5H_5NH)_2[PbCl_6]$, vs. temperature.

$Cl^{(2)}$, the other two directions point towards $Cl^{(3)}$ of two different $[SnCl_6]$ octahedra. In the projection onto the ac-plane the octahedra at 0, 0, 0 coincide with the centered at 0, 1, 0. The connections H ... Cl marked in Fig. 5 by points go from pyridinium ring within the cell to the octahedra centered at 0, 1, 0, whereas the dashed ones go to the octahedra at 0, 0, 0. In this way hydrogen bonded strings $[SnCl_6] \cdot [C_5H_6N]$ run along ***a***, and these strings may interact via van der Waals forces between the pyridinium rings to form planes (0, 1, 1). The pyridinium rings are nearly planar with a maximum deviation of 1 pm from the best plane through the carbon and nitrogen atoms. The planarity is also seen from the sum of the bond angles C−C−C, C−N−C and N−C−C, which is 720°, see Table 4. The trifurcated hydrogen bond system N−H ... $\{Cl^{(2)}, Cl^{(3)}, Cl^{(3)}\}$ forms a axially distorted tetrahedron with angles N−H ... Cl of 124° ± 3° (see Table 9). In Fig. 6 the projection of

Table 5. Unit cell dimensions of the high (I) and low temperature (II) phases of bis(pyridinium)hexachlorometallates $(C_5H_5NH)_2[MCl_6]$, M = Sn, Te, Pb, Pt. The monoclinic high temperature phase (I), space group C^2_{2h}-B2/m, $Z = 2$, was transformed to a triclinic cell, $(P\bar{1})_{tr}$, $Z = 1$. – [a] Determination at room temperature [6].

M	Phase	Space group	a/pm	b/pm	c/pm	α/°	β/°	γ/°	$V/(10^6\,\mathrm{pm}^3)$	T/K
Sn	I	B2/m	1294	800	838	90	90	96.12	859.5	338
	I	$(P\bar{1})_{tr}$	771	798	771	84.87	65.86	84.87	429.8	338
	II	$P\bar{1}$	734.1	799.0	799.7	83.229	65.377	84.387	422.8	297
Pb	I	B2/m	1297	802	839	90	90	96.52	866.9	338
	I	$(P\bar{1})_{tr}$	772	802	772	84.53	65.78	84.53	433.4	338
	II	$P\bar{1}$	743	799	798	83.53	65.65	84.29	427.6	293
Pt	I	B2/m	1330	788	809	90	90	92.93	846.6	338
	I	$(P\bar{1})_{tr}$	778	788	778	87.50	62.59	87.50	423.3	338
	II	$P\bar{1}$	747	794	804	85.13	62.40	88.17	421.5	283
Te	I	B2/m	1288.2	800.4	847.0	90	90	96.82	867.1	[a]

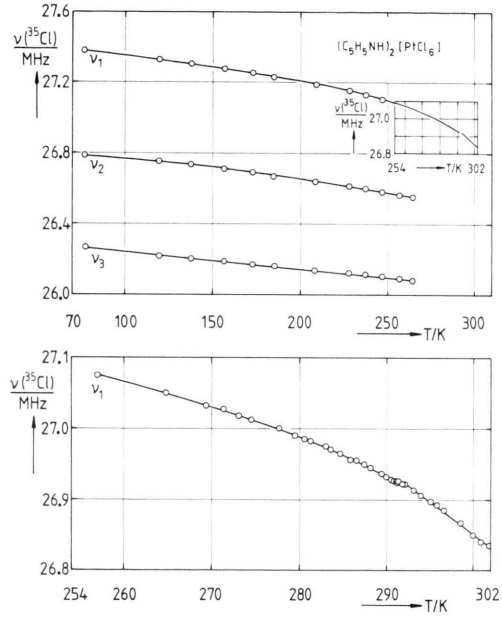

Fig. 4. ^{35}Cl NQR frequencies of bis(pyridinium)hexachloroplatinate $(C_5H_5NH)_2[PtCl_6]$ vs. temperature. ν_1 is shown around T_c in an enlarged scale.

the unit cell of $(C_5H_5NH)_2[SnCl_6]$, Phase II, along $\boldsymbol{c}$ is shown. During the phase transition the triclinic cell, space group C_1^1-$P\bar{1}$, $Z = 1$, transforms into a monoclinic unit cell, space group C^2_{2h}-B2/m, $Z = 2$. In Fig. 7 we show the triclinic cell of phase II in projection along [010], from which the orthorhombic cell B2/m is easily seen (with a slight deviation in the angle β from 90°). The transformation I → II is given by $\boldsymbol{a}(\mathrm{II}) = (\boldsymbol{a}(\mathrm{I}) + \boldsymbol{c}(\mathrm{I}))/2$, $\boldsymbol{b}(\mathrm{II}) = \boldsymbol{b}(\mathrm{I})$, $\boldsymbol{c}(\mathrm{II}) = (\boldsymbol{c}(\mathrm{I}) - \boldsymbol{a}(\mathrm{I}))/2$, $V(\mathrm{II}) = V(\mathrm{I})/2$. In Table 5 we have

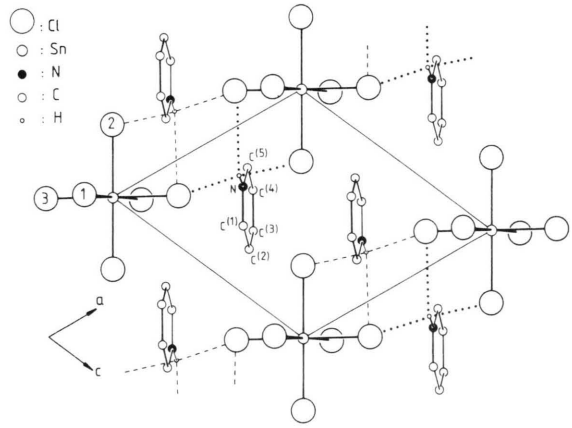

Fig. 5. Projection of the unit cell onto the ac-plane including the hydrogen bond scheme (see Table 9). In this figure, as in the following ones, the hydrogen atoms bonded to carbon atoms are omitted.

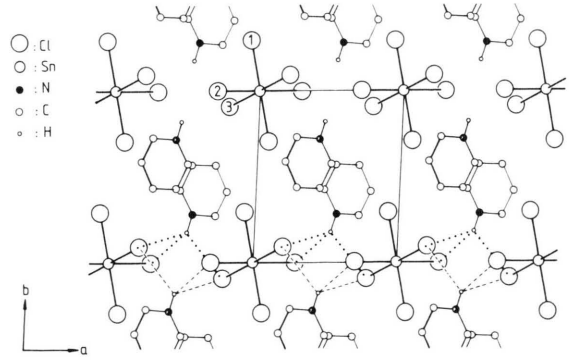

Fig. 6. Projection of the crystal lattice along $\boldsymbol{c}$; the pointed connections H ... Cl go from a pyridinium ring below the ab-plane, the dashed connections from a pyridinium ring above the ab-plane to the octahedra centered in the ab-plane.

Table 6. Power series expansion of $\nu(^{35}Cl) = f(T) = \sum a_i T^i$ for bis(pyridinium)hexachlorometallates $(C_5H_5NH)_2[MCl_6]$, M = Sn, Te, Pb, Pt and $(C_5H_5ND)_2[SnCl_6]$ and $(C_5D_5NH)_2[SnCl_6]$. Z = number of experimental points used for the fitting. σ is the standard deviation and $\Delta T = T_1 \ldots T_2$ is the temperature range for which the polynom $\sum a_i T^i$ was fitted to the experiment.

M	^{35}Cl NQR line	Z	$\sigma \cdot 10^3$ / MHz	a_{-1} / MHz · K	a_0 / MHz	$a_1 \cdot 10^4$ / MHz · K^{-1}	$a_2 \cdot 10^6$ / MHz · K^{-2}	ΔT / K
Sn [a]	ν_3	16	2.2	−12.2570	15.6230	−22.9546	5.4688	77 ... 294
	ν_2	16	3.0	11.9123	17.0125	16.3219	−7.9407	77 ... 294
	ν_1	26	2.3	8.2661	17.4032	12.8507	−4.8846	77 ... 294
	ν_1	21	1.7	3364.7089	−19.6929	1369.1933	−169.2067	295 ... 332
	ν_1	7	0.8	–	18.1518	−27.2862	–	333 ... 349
Sn [b]	ν_3	16	2.9	−7.6335	15.5099	−14.6470	3.9621	77 ... 288
	ν_2	16	3.2	13.4669	16.9964	17.6713	−8.2178	77 ... 288
	ν_1	16	2.2	11.3409	17.3477	15.2941	−5.2781	77 ... 288
	ν_1	13	1.2	529.8872	9.3315	382.9525	−58.0686	289 ... 330
	ν_1	8	2.0	–	18.1348	−26.8324	–	331 ... 345
Sn [c]	ν_3	17	2.6	−12.4666	15.6216	−23.2241	5.5820	77 ... 295
	ν_2	17	4.9	16.1200	16.9237	22.1392	−9.0593	77 ... 295
	ν_1	17	3.5	12.1000	17.3235	18.0839	−5.8482	77 ... 295
	ν_1	17	2.7	1773.5251	−6.2037	995.1016	−135.4561	296 ... 330
	ν_1	8	1.2	–	18.1467	−27.0594	–	331 ... 349
Te [a]	ν_3	12	2.0	−7.3267	16.0950	−17.8088	3.9244	77 ... 250
	ν_2	12	1.7	10.9762	15.7983	21.2623	−6.6324	77 ... 250
	ν_1	12	1.3	6.2384	16.6346	22.6534	−9.3012	77 ... 250
	ν_1	5	2.4	771.2081	5.2217	568.5032	−94.0248	251 ... 271
	ν_1	17	2.7	–	17.2132	−24.4330	–	272 ... 328
Pb [a]	ν_3	15	4.9	−26.4437	16.4784	−51.0774	12.9625	77 ... 299
	ν_2	15	9.1	23.7364	19.4943	45.3185	−18.3272	77 ... 299
	ν_1	15	5.4	6.6376	19.3899	18.1824	−5.8402	77 ... 299
	ν_1	9	0.8	−2443.4602	30.2013	100.0525	−62.6440	300 ... 319
	ν_1	17	2.4	–	20.4044	−32.9066	–	320 ... 360
Pt [a]	ν_3	13	2.8	12.7113	26.0619	7.9848	−3.3647	77 ... 265
	ν_2	13	2.6	0.2195	26.8223	−2.3884	−2.9676	77 ... 265
	ν_1	13	4.1	14.8077	27.0923	19.5761	−8.7164	77 ... 265
	ν_1	20	1.5	−421.0531	26.8314	221.7895	−58.0191	266 ... 291
	ν_1	16	3.0	–	29.3630	−83.6173	–	292 ... 303

[a] Cation: $(C_5H_5NH)^{\oplus}$, [b] Cation: $(C_5H_5ND)^{\oplus}$. [c] Cation: $(C_5D_5NH)^{\oplus}$.

compared the dimensions of the high temperature phase, transformed into C_i^1-$P\bar{1}$, $Z = 1$, with the dimensions of phase II.

Going through T_c from phase II to phase I, $|\boldsymbol{a}|$ increases slightly ($\approx 4\%$) whereas $|\boldsymbol{c}|$ decreases by about the same amount. $|\boldsymbol{b}|$ is practically unchanged as are the angles α, β and γ. The overall effect is seen by comparing the volumes V(I) with the volumes V(II). The difference in temperatures at which the unit cells of the phases I and II have been determined, $\Delta T \approx 40-45\,^{\circ}C$, results in a ΔV of 0.5 to 1.8%, being smallest for the Pt-compound and largest for the Pb-salt. The very small shifts in the mutual contacts of the ions in the lattice by passing T_c is reflected in ΔH(transition); we have not been able to detect it by differential thermal analysis for any of the four compounds.

The octahedron $[SnCl_6]$ conserves its symmetry $\bar{1}$ during the transition I ↔ II, e.g. there are three crystallographically inequivalent Cl-atoms within the octahedra in both phases. In phase I, a mirror plane perpendicular to the ring C_5H_6N makes the atoms $C^{(1)}$ and N, $C^{(3)}$ and $C^{(4)}$ and $C^{(2)}$ and $C^{(5)}$ equivalent. Therefore the symmetry shows that in the high temperature phase the pyridinium ion either rotates around an axis perpendicular to the ring plane or a flipping motion around this axis with a period of $n \cdot 60\,^{\circ}$ occurs. X-ray diffraction or neutron diffraction can not distinguish between these two modes because the time scales of the

Table 7. ^{35}Cl-NQR frequencies ν_i/MHz of bis(pyridinium)hexachlorometallates $(C_5H_5NH)_2[MCl_6]$, M = Sn, Te, Pb, Pt, $(C_5H_5ND)_2[SnCl_6]$ and $(C_5D_5NH)_2[SnCl_6]$ at selected temperatures. The mean error of the frequency is ± 0.005 MHz. The signal to noise (S/N) ratio is determined with lock-in technique, time constant 10 s.

M	^{35}Cl NQR line	T = 77 K	S/N	T = 200 K	S/N	T = 250 K	S/N	T = 300 K	S/N	T = 350 K	S/N
Sn [a]	ν_3	15.320	9	15.321	30	15.341	25	–	–	–	–
	ν_2	17.245	8	17.080	30	16.971	25	–	–	–	–
	ν_1	17.580	8	17.506	30	17.452	25	17.371	25	17.196	2
Sn [b]	ν_3	15.320	4	15.337	7	15.360	7	–	–	–	–
	ν_2	17.258	5	17.088	7	16.978	7	–	–	–	–
	ν_1	17.580	4	17.499	7	17.445	7	17.359	8	17.194	2
Sn [c]	ν_3	15.315	8	15.318	30	15.340	30	–	–	–	–
	ν_2	17.245	9	17.084	30	16.975	50	–	–	–	–
	ν_1	17.585	8	17.511	30	17.453	40	17.371	40	17.199	2
Te [a]	ν_3	15.886	3	15.859	7	15.865	2	–	–	–	–
	ν_2	16.065	3	16.012	10	15.958	2	–	–	–	–
	ν_1	16.835	3	16.746	10	16.644	8	16.480	5	–	–
Pb [a]	ν_3	15.820	5	15.846	20	15.902	25	–	–	–	–
	ν_2	20.040	5	19.775	20	19.576	25	–	–	–	–
	ν_1	19.580	5	19.553	20	19.506	25	19.424	15	19.253	8
Pt [a]	ν_3	26.269	8	26.150	10	26.102	10	–	–	–	–
	ν_2	26.789	8	26.656	10	26.577	10	–	–	–	–
	ν_1	27.383	8	27.209	10	27.096	10	26.849	5	–	–

[a] Cation $(C_5H_5NH)^{\oplus}$; [b] Cation $(C_5H_5ND)^{\oplus}$; [c] Cation $(C_5D_5NH)^{\oplus}$.

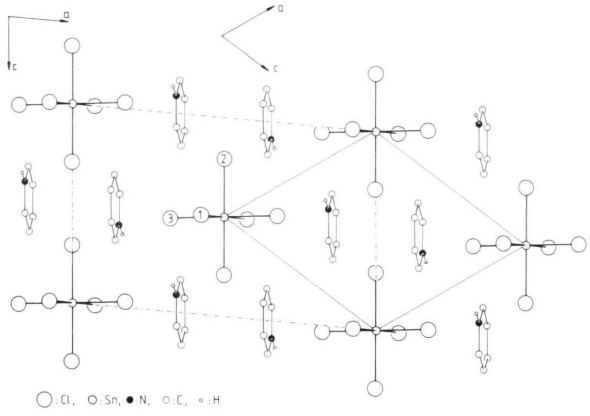

Fig. 7. Projection of unit cell along ***b***. The interrupted lines show the base of a B-centered triclinic cell with $Z = 2$, which is changed into a B-centered monoclinic cell, space group B2/m, $Z = 2$, at T_c.

Table 8. Temperatures $T_c = T_{I \rightleftarrows II}$ of the phase transitions high temperature phase I ⇄ II low temperature phase II for bis(pyridinium)hexachlorometallates, found from the NQR frequencies $\nu(^{35}Cl) = f(T)$.

Compound	T_c/K
$(C_5H_5NH)_2[SnCl_6]$	332.0
$(C_5H_5ND)_2[SnCl_6]$	330.0
$(C_5D_5NH)_2[SnCl_6]$	330.4
$(C_5H_5NH)_2[TeCl_6]$	272.3
$(C_5H_5NH)_2[PbCl_6]$	319.5
$(C_5H_5NH)_2[PtCl_6]$	291.0

diffraction experiments and of the librational motion are incommensurable.

^{35}Cl NQR Spectroscopy

At 77 K each of the bis(pyridinium)hexachlorometallates(IV) shows in the ^{35}Cl NQR spectrum three lines of equal intensity. This observation is in agreement with the three crystallographically inequivalent Cl-atoms in the low temperature phase $P\bar{1}$, $Z = 1$. With increasing temperature two of the three lines fade out and for the remaining one $d\nu(^{35}Cl)/dT$ becames more negative. For this line, $d\nu(^{35}Cl)/dT$ changes discontinuously at the transition temperature T_c and $d^2\nu(^{35}Cl)/dT^2$ is almost zero above T_c. This behaviour of $\nu(^{35}Cl) = f(T)$ is qualitatively the same for the four pyridinium salts studied here. On comparing $\nu(^{35}Cl)$ of $(C_5H_5ND)_2[SnCl_6]$ with $\nu(^{35}Cl)$ of $(C_5H_5NH)_2[SnCl_6]$,

Table 9. Hydrogen bond distances and angles in bis(pyridinium)hexachlorostannate, phase II. N at $x = 0.4323$, $y = 0.7185$, $z = 0.2552$; H at $x = 0.4659$, $y = 0.8212$, $z = 0.2019$; $Cl^{(2)}$ at $x = 0.2922$, $y = -0.0018$, $z = -0.2892$; $Cl^{(3)}$ at $x = 0.2050$, $y = 0.0922$, $z = 0.1457$.

Atom (coord.)	atom (coord.) ..... atom (coord.)		Sn on plane	N ... Cl	H ... Cl	N–H ... Cl
				pm	pm	degrees
$N(x, y, z)$	$-H(x, y, z)$	... $Cl^{(2)}(1-x, 1-y, -z)$	(110)	328.6	274.0	121
		... $Cl^{(3)}(x, 1+y, z)$	(010)	347.7	287.0	127
		... $Cl^{(3)}(1-y, 1-y, -z)$	(110)	349.1	288.4	127
$N(1-y, 1-y, 1-z)$	$-H(1-x, 1-y, 1-z)$	... $Cl^{(2)}(x, y, 1+z)$	(001)	328.6	274.0	121
		... $Cl^{(3)}(1-x, -y, 1-z)$	(101)	347.7	287.0	127
		... $Cl^{(3)}(x, y, 1+z)$	(001)	349.1	288.4	127

Table 10. ^{35}Cl NQR frequency shift of $(C_5H_5ND)_2[SnCl_6]$ and $(C_5D_5NH)_2[SnCl_6]$ with respect to $(C_5H_5NH)_2[SnCl_6]$. $\Delta\nu_i = \nu_i(C_5H_5ND)_2[SnCl_6] - \nu_i(C_5H_5NH)_2[SnCl_6]$ (upper part of the table); $\Delta\nu_i = \nu_i(C_5D_5NH)[SnCl_6] - \nu_i(C_5H_5NH)_2[SnCl_6]$ (lower part of the table).

	77 K → 295 K	295 K → 325 K	330 K → 350 K
$(C_5H_5ND)_2[SnCl_6]$			
$\Delta\nu_1$/kHz	0 → −7	−7 → 12	−2
$\Delta\nu_2$/kHz	13 → 5	–	–
$\Delta\nu_3$/kHz	0 → 18	–	–
$(C_5D_5NH)_2[SnCl_6]$			
$\Delta\nu_1$/kHz	0 → 5	5 → −6	+3
$\Delta\nu_2$/kHz	0 → 4	–	–
$\Delta\nu_3$/kHz	−5 → 0	–	–

an interesting result is found. For the two lines on the lower part of the frequency scale, deuteration at the nitrogen site leads to an increase in frequency, and for the high frequency line – the one which persists into phase I – the opposite is true. In Table 10 these isotope induced frequency shifts are listed. The effect of deuteration, going in different directions, is of some help in assigning hydrogen bonds to certain atoms in the unit cell [16]. In the problem discussed here, two of the Cl-atoms out of the three crystallographically inequivalent ones have something to do with a hydrogen bond N–H ... Cl, while the third Cl-atom is practically not influenced by hydrogen bonding.

When looking on Tables 4 and 9 and Figs. 5 and 6, one finds that it is $Cl^{(2)}$ which is connected by two short hydrogen contacts with two different ions $(C_5H_5NH)^+$, and its distance to the central atom M^{IV} is the longest one in the list of d(Sn–Cl). An increasing distance d(Sn–Cl) can be related to increasing ionic character of the bond Sn–Cl, which in the frame of Townes-Dailey theory [17] leads to a decrease of ^{35}Cl NQR frequencies. Taking the Ubbelohde effect, see [18], into account according to which in O–H(D) ... O systems the O–D bond is normally shorter than the O–H bond and transferring this effect to bonds N–H(D) ... Cl, the distance D ... Cl will be longer than H ... Cl. This means that the hydrogen bond in the protonated system is stronger and the corresponding ^{35}Cl NQR frequency lower than in the deuterated species. Such a behaviour was observed for the ethylenediammonium hexachlorometallates [3]. The middle one of the ^{35}Cl NQR lines in the low temperature triplett is somewhat differently influenced by an exchange H → D. We ascribe the line ν_2 to the atom $Cl^{(2)}$. It is interesting to note that the H → D effect on $\nu(^{35}Cl^{(2)})$ decreases with increasing temperature while the opposite is observed for $\nu(^{35}Cl^{(3)})$. The atom $Cl^{(1)}$ is not incorporated in the hydrogen bond system. The highest ^{35}Cl NQR frequency belongs to it. Whereas the lines $\nu(^{35}Cl^{(2)})$ and $\nu(^{35}Cl^{(3)})$ show a fade out, the atom $Cl^{(1)}$ is not influenced by the dynamics of the trifurcated hydrogen bond system. The assignment proposed here, $\nu_1(^{35}Cl) \leftrightarrow Cl^{(1)}$, $\nu_2(^{35}Cl) \leftrightarrow Cl^{(2)}$ and $\nu_3(^{35}Cl) \leftrightarrow Cl^{(3)}$ is based on qualitative arguments. Single crystals Zeeman split NQR spectroscopy, see e.g. [19], would give a unique assignment.

The lowering of T_c by deuteration of a system R–N–H ... Halogen was observed several times [20, 21, 22]. The shifts of the ^{35}Cl NQR frequency

due to the ring deuteration, $C_5H_5NH \rightarrow C_5D_5NH$ is smaller than the shifts due to the exchange $C_5H_5NH \rightarrow C_5H_5ND$, and the difference is more pronounced for ν_2 and ν_3 than for ν_1. The exchange $C_5H_5NH \rightarrow C_5D_5NH$ is mainly affecting the lattice dynamics via the lower lying rotational-vibrational modes.

Acknowledgement

We gratefully acknowledge the support of this work by the Deutsche Forschungsgemeinschaft. – We also thank Dr. H. Paulus for collecting the single crystal X-ray diffraction data and B. Baumgartner for the help with the powder diffraction experiments.

[1] D. Nakamura, Bull. Chem. Soc. Japan **36,** 1162 (1963).
[2] L. Ramakrishnan, S. Soundararajan, V. S. S. Sastry, and J. Ramakrishna, Coord. Chem. Rev. **22,** 123 (1977).
[3] D. Borchers and Al. Weiss, Ber. Bunsenges. Phys. Chem. **90,** 718 (1986).
[4] T. B. Brill and W. A. Welsh, J. Chem. Soc. Dalton Trans. **1973,** 357.
[5] E. E. Aynsley and A. C. Hazell, Chem. and Ind. **1969,** 611.
[6] P. P. Khodadad, B. Viossat, P. Toffoli, and N. Rodier, Acta Cryst. **B 35,** 2896 (1979).
[7] C. W. Gould and S. T. Gross, Anal. Chem. **25,** 749 (1953).
[8] H. Hartl, Acta Cryst. **B 31,** 1781 (1975).
[9] R. F. Copeland, S. H. Conner, and E. A. Meyers, J. Phys. Chem. **70,** 1288 (1966).
[10] A. J. Serewicz, B. K. Robertson, and E. A. Meyers, J. Phys. Chem. **69,** 1915 (1965).
[11] P. C. Rérat, Acta Cryst. **15,** 427 (1962).
[12] R. Weinland and E. Bames, Z. anorg. Chem. **62,** 260 (1909).
[13] A. Gutbier and F. Flury, J. prakt. Chem. **86,** 150 (1912).
[14] A. Gutbier and M. Wissmueller, J. prakt. Chem. **90,** 491 (1914).
[15] P. Groth, Chemische Krystallographie, Vol. 5, Verlag W. Engelmann, Leipzig 1919.
[16] W. Pies and Al. Weiss, Advances in NQR **1,** 57 (1974).
[17] C. H. Townes and B. P. Dailey, J. Chem. Phys. **17,** 782 (1949).
[18] W. C. Hamilton and J. A. Ibers, in: Hydrogen Bonding (W. A. Benjamin, ed.). New York 1968, p. 104.
[19] V. Nagarajan, H. Paulus, N. Weiden, and Al. Weiss, J. Chem. Soc. Faraday Trans. 2, **82,** 1499 (1986).
[20] W. Pies and Al. Weiss, Bull. Chem. Soc. Japan **51,** 1051 (1978).
[21] G. Fecher and Al. Weiss. Ber. Bunsenges. Phys. Chem. **90,** 10 (1986).
[22] V. G. Krishnan and Al. Weiss, J. Mol. Struct. **111,** 379 (1983).